

Density of excess modes below the first phonon mode in four-dimensional glasses

Lijin Wang(王利近), Ding Xu(胥鼎), and Shiyun Zhang(张世允)

Citation: Chin. Phys. B, 2024, 33 (**7**): 076401. DOI: 10.1088/1674-1056/ad3dd1
Journal homepage: http://cpb.iphy.ac.cn; http://iopscience.iop.org/cpb

What follows is a list of articles you may be interested in

K-core attack, equilibrium *K*-core, and kinetically constrained spin system

Hai-Jun Zhou(周海军)
Chin. Phys. B, 2024, 33 (**6**): 066402. DOI: 10.1088/1674-1056/ad4329

Low-frequency hybridized excess vibrations of two-dimensional glasses

Licun Fu(付立存), Yiming Zheng(郑一鸣), and Lijin Wang(王利近)
Chin. Phys. B, 2024, 33 (**5**): 056401. DOI: 10.1088/1674-1056/ad205e

Quench dynamics in 1D model with 3rd-nearest-neighbor hoppings

Shuai Yue(岳帅), Xiang-Fa Zhou(周祥发), and Zheng-Wei Zhou(周正威)
Chin. Phys. B, 2021, 30 (**2**): 026402. DOI: 10.1088/1674-1056/abd742

Characteristics of phase transitions via intervention in random networks

Jia Xiao (贾啸), Hong Jin-Song (洪劲松), Yang Hong-Chun (杨宏春), Yang Chun (杨春), Shi Xiao-Hong (史晓红), Hu Jian-Quan (胡建全)
Chin. Phys. B, 2014, 23 (**7**): 076401. DOI: 10.1088/1674-1056/23/7/076401

Simulations of the flipping images and microparameters of molecular orientations in liquids according to molecule string model

Wang Li-Na (王丽娜), Zhao Xing-Yu (赵兴宇), Zhang Li-Li (张丽丽), Huang Yi-Neng (黄以能)
Chin. Phys. B, 2012, 21 (**8**): 086403. DOI: 10.1088/1674-1056/21/8/086403

Density of excess modes below the first phonon mode in four-dimensional glasses

Lijin Wang(王利近)[1,†], Ding Xu(胥鼎)[2,‡], and Shiyun Zhang(张世允)[2,§]

[1] *School of Physics and Optoelectronic Engineering, Anhui University, Hefei* 230601, *China*
[2] *Department of Physics, University of Science and Technology of China, Hefei* 230026, *China*

(Received 22 February 2024; revised manuscript received 2 April 2024; accepted manuscript online 12 April 2024)

Glasses are known to possess low-frequency excess modes beyond the Debye prediction. For decades, it has been assumed that evolution of low-frequency density of excess modes $D(\omega)$ with frequency ω follows a power-law scaling: $D(\omega) \sim \omega^{\gamma}$. However, it remains debated on the value of γ at low frequencies below the first phonon-like mode in finite-size glasses. Early simulation studies reported $\gamma = 4$ at low frequencies in two- (2D), three- (3D), and four-dimensional (4D) glasses, whereas recent observations in 2D and 3D glasses suggested $\gamma = 3.5$ in a lower-frequency regime. It is uncertain whether the low-frequency scaling of $D(\omega) \sim \omega^{3.5}$ could be generalized to 4D glasses. Here, we conduct numerical simulation studies of excess modes at frequencies below the first phonon-like mode in 4D model glasses. It is found that the system size dependence of $D(\omega)$ below the first phonon-like mode varies with spatial dimensions: $D(\omega)$ increases in 2D glasses but decreases in 3D and 4D glasses as the system size increases. Furthermore, we demonstrate that the $\omega^{3.5}$ scaling, rather than the ω^4 scaling, works in the lowest-frequency regime accessed in 4D glasses, regardless of interaction potentials and system sizes examined. Therefore, our findings in 4D glasses, combined with previous results in 2D and 3D glasses, suggest a common low-frequency scaling of $D(\omega) \sim \omega^{3.5}$ below the first phonon-like mode across different spatial dimensions, which would inspire further theoretical studies.

Keywords: vibrational density of states, excess modes, four-dimensional glasses, scaling, computer simulation

PACS: 64.70.Q–, 64.70.kj **DOI:** 10.1088/1674-1056/ad3dd1

1. Introduction

The presence of disorder endows glasses with a variety of exotic properties that distinguish them from their crystalline counterparts. One mysterious but universal hallmark of glasses is that there exist excess vibrational modes at low frequencies ω. These excess modes (also termed non-phononic or quasi-localized modes) are beyond the prediction of Debye theory,[1] which expects that the low-frequency density of vibrational modes $\mathcal{D}(\omega) = A_{\mathrm{D}}\omega^{d-1}$, with d being the spatial dimension and A_{D} the Debye level given by Debye theory. Interestingly, in addition to the initial idea of resorting to excess modes to rationalize the anomalous temperature dependence of thermodynamic properties,[2–5] numerous studies over the last two decades have demonstrated that excess modes could also shed light on deciphering other mysterious peculiarities of glasses and glass transition.[6–19] For example, soft spots defined from low-frequency excess modes show strong spatial correlation with those particles exhibiting larger rearrangements upon deformations or thermal excitations;[8,11,12,15] the glass transition could be understood from low-frequency properties of excess modes;[14,16] the strength of sound attenuation due to disorder in glasses correlates closely with the low-frequency density of excess modes.[17–19] However, understanding of low-frequency excess modes themselves still remains far from satisfactory.

One subject of intense debate up to date is how the density of excess modes $D(\omega)$ evolves with ω. In the literature, it is assumed that $D(\omega)$ follows a power law, $D(\omega) \sim \omega^{\gamma}$. However, the value of the scaling exponent γ is still under debate. There have been some theoretical efforts on this, and relevant theories or phenomenological models[20–29] predicted that γ could be 2, 3, or 4. Nevertheless, the inconsistency on the value of γ in different theoretical frameworks has not yet been reconciled.

Nowadays, computer simulations make it possible to directly determine spectra of excess modes in large model glass formers. However, when the system size is large enough, glasses as well as crystals would behave like a continuum elastic medium,[30–32] and the frequencies of low-frequency excess modes will converge to those of phonon-like modes (also termed extended modes), hence resulting in the hybridization of excess modes and phonon-like modes. The mode hybridization poses great difficulties in the numerical determination of the spectrum of excess modes, because one has to conceive effective ways to distinguish between excess modes and phonon-like modes. To deal with the hybridization problem, several ideas have been proposed recently.

One approach is to separate modes by presetting a thresh-

[†]Corresponding author. E-mail: lijin.wang@ahu.edu.cn
[‡]Corresponding author. E-mail: dingxu@mail.ustc.edu.cn
[§]Corresponding author. E-mail: zsy12@mail.ustc.edu.cn

© 2024 Chinese Physical Society and IOP Publishing Ltd

old of participation ratio, given that the participation ratio of excess modes usually takes smaller values than phonon-like modes.[33,34] For excess modes hybridizing with phonon-like modes, this approach could lead to $D(\omega) \sim \omega^4$ in three-dimensional (3D) systems; however, it could not work well in two-dimensional (2D) systems where there are very few or even no excess modes at very low frequencies.[33] Subsequently, Wang *et al.*[17] obtained the density of excess modes by subtracting the Debye contribution from the total density of states, and found that $D(\omega) \sim \omega^2$ in 2D glasses while $D(\omega) \sim \omega^4$ in 3D glasses. The quartic scaling of the density of excess modes in 3D glasses agrees with what has been reported from separating the modes using the participation ratio cutoff.[33,34] Additionally, there are more other methods proposed in recent years to de-hybridize between the excess modes and phonon-like modes, e.g., the nonlinear mode method,[35] the augmented potential method,[36] and the pinning method.[37–39]

The frequency of the first phonon-like mode could be given by $\omega_1 = \sqrt{G/\rho}(2\pi/L)$, where G, ρ, and L are the shear modulus, the mass density, and the liner size of the system, respectively. Therefore, when the system size (or L) becomes smaller, ω_1 will be pushed to a higher frequency, thus leaving below ω_1 a low-frequency window where only excess modes dwell.[40] It is then straightforward to assume that the density of excess modes is equal to the total density of vibrational modes at frequencies significantly below ω_1. Following this line of research, there have been numerous numerical studies[17,40–44] focusing on the spectrum of excess modes below ω_1.

Early numerical studies[40,41,44] argued that $D(\omega) \sim \omega^\gamma$ with $\gamma = 4$ at low frequencies below ω_1 in 3D systems, which is in agreement with the results from studying excess modes hybridizing with phonon-like modes.[17,33,34] Moreover, it has also been argued that the quartic scaling could be generalized to 2D and four-dimensional (4D) glasses.[41,43,45] However, the universality of the quartic scaling of the excess-mode spectrum below ω_1 has recently been challenged by some simulation studies[17,42,43,46–51] in both 2D and 3D glasses. Of these studies reporting the deviations from the low-frequency ω^4 distribution, in Refs. [17,48,49] researchers reported that $\gamma = 3.5$ in a low-frequency regime far below ω_1 in both 2D and 3D glasses, regardless of the system size and interaction potential model. In addition, the ω^4 and $\omega^{3.5}$ scalings could even be observed simultaneously in some glasses but appear in different frequency regimes: the $\omega^{3.5}$ scaling, when compared to the ω^4 one, appears in a lower-frequency regime. Then, it is interesting to check whether the scenario of the $\omega^{3.5}$ scaling of the excess-mode spectrum observed in both 2D and 3D glasses could persist as well in 4D glasses.

In this work, we numerically investigate the density of excess modes below the first phonon-like mode in 4D model glasses with different system sizes, and probe frequencies down to values as small as possible by resorting to extremely large ensemble sizes. First, we show that the system size N dependence of the density of excess modes below the first phonon-like mode in 2D glasses is different from those in both 3D and 4D glasses. Second, we demonstrate that a low-frequency $\omega^{3.5}$ scaling of the excess-mode spectrum observed previously in both 2D and 3D glasses works well in 4D glasses, thus suggesting the universality of this scaling across different spatial dimensions (at least when d takes values of 2, 3, and 4).

2. Simulation details

We conducted numerical simulations in two well-studied model glass-forming systems in 4D, which are both composed of a 50 : 50 binary mixture of A particles and B particles with equal mass. Note that 4D refers to the dimensionality being 4. The 4D simulations incorporate an additional axis, referred to as, e.g., the h-axis here, alongside the commonly used x-, y-, and z-axes in 3D. Any two of the four axes in 4D are set to be mutually perpendicular, and particles along the h-axis possess properties such as positions and velocities, as in any other axis.

(I) In the inverse power law (IPL) potential model, the interaction between two particles i and j is $V(r_{ij}) = [(\frac{\sigma_{ij}}{r_{ij}})^{10} + c_0 + c_2(\frac{r_{ij}}{\sigma_{ij}})^2 + c_4(\frac{r_{ij}}{\sigma_{ij}})^4]H(r_{ij}^c - r_{ij})$. Here, $H(r)$ is the Heaviside step function, r_{ij} is the particle separation, $\sigma_{\rm AA} = 1.0$, $\sigma_{\rm BB} = 1.4$, and $\sigma_{\rm AB} = 1.18$. The constants c_0, c_2, and c_4 could make continuous the first and second derivatives of $V(r_{ij})$ at the interaction cutoff $r_{ij}^c = 1.48\sigma_{ij}$. The number density $n = N/L^4$ in 4D is chosen to be 0.80.

(II) In the harmonic (HARM) potential model, $V(r_{ij}) = \frac{1}{2}(1 - \frac{\sigma_{ij}}{r_{ij}})^2 H(\sigma_{ij} - r_{ij})$, where $\sigma_{\rm AA} = 1.0$, $\sigma_{\rm BB} = 1.4$, and $\sigma_{\rm AB} = 1.2$. The pressure is held to be 0.01 in 4D.

We generated zero-temperature ($T = 0$) glasses by quenching instantaneously very high-temperature liquids via energy minimization[52] to their inherent structures, and these $T = 0$ glasses are thus poorly annealed. We obtained vibrational modes by diagonalizing dynamical matrix of $T = 0$ glasses. To avoid the binning issue (see Ref. [48] for a detailed description) in the calculation of density of states given by $D(\omega) = \frac{1}{dN-d}\sum_{l=1}^{dN-d}\delta(\omega - \omega_l)$ with ω_l being the eigenfrequency of the l-th mode, we calculated instead the cumulative density of states, $I(\omega) = \int_0^\omega D(\omega')\,{\rm d}\omega'$, by counting the number of modes up to ω. We will show mainly systematic results obtained from the IPL model, and some results from the HARM model will be presented.

3. Results and discussion

There are usually two types of excess modes in the literature:[33,35,40] one is excess modes hybridizing with phonon-like modes; the other is excess modes not hybridizing with phonon-like modes, e.g., excess modes below the first phonon-like mode ω_1. In this work, we focus particularly on excess modes below ω_1 in 4D glasses. As for excess modes hybridizing with phonon-like modes in 4D glasses, we leave it for a future study.

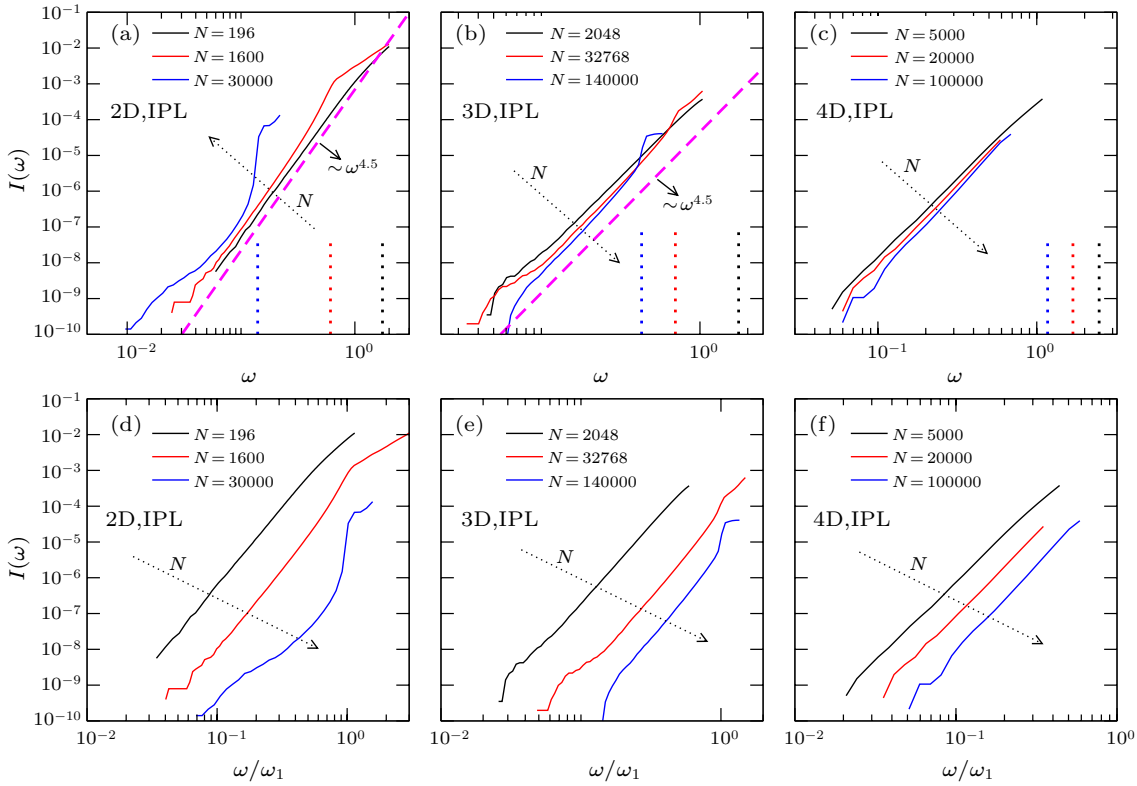


Fig. 1. Finite-size effects on the cumulative density of states $I(\omega)$ in 2D (a), 3D (b), and 4D (c) IPL model glasses. Each vertical dotted line marks approximately the frequency of the first phonon-like mode $\omega_1 = \sqrt{G/\rho}(2\pi/L)$, where the shear modulus G was determined by taking the average over different samples. Specifically, the vertical dotted lines from right to left: (a) for $N = 196$, $N = 1600$, and $N = 30000$; (b) for $N = 2048$, $N = 32768$, and $N = 140000$; (c) for $N = 5000$, $N = 20000$, and $N = 100000$. Some data in 2D and 3D IPL model glasses are taken from Refs. [17,48,49], to which we refer for further simulation details. One could observe that $I(\omega)$ at frequencies far below ω_1 in 2D glasses increases with increasing N, whereas the N dependence of $I(\omega)$ at frequencies far below ω_1 in both 3D and 4D glasses behaves oppositely from that in 2D glasses. For reference, in (d), (e) and (f) are $I(\omega)$ versus the reduced frequency ω/ω_1 for the same data as in (a), (b) and (c), respectively.

We present in Fig. 1 how spatial dimensions influence the dependence of the cumulative density of excess modes $I(\omega)$ on system sizes. As shown in Fig. 1(a) for 2D glasses, $I(\omega)$ at frequencies below ω_1 increases with increasing N, suggesting that there are more excess modes in a larger 2D system, which is consistent with previous numerical studies.[41,49] This is also in line with the prediction from a theoretical study[41,53] based on the continuity elasticity, see Refs. [46,49] for a detailed comparison between the simulation and theory.

Next, we turn to check how $I(\omega)$ at frequencies below ω_1 evolves with N in 3D and 4D glasses. From the numerical results presented in Fig. 2 of Ref. [41], one could conclude that there are nearly no finite-size effects on $I(\omega)$ in 3D IPL model glasses when N changes from 1000 to 4000 and also in 4D IPL model glasses when N changes from 5000 to 20000. However, it was reported subsequently that the scaling of the low-frequency $I(\omega)$ suffers from finite-size effects in 3D glasses.[42] This thus implies that there should be a finite-size effect on $I(\omega)$ in 3D glasses, but it is unclear whether $I(\omega)$ increases with increasing N in 3D glasses as it does in 2D glasses. This motivates us to revisit the N dependence of $I(\omega)$ in both 3D and 4D glasses by probing frequencies down to very small values. What unexpected is that the N dependence of $I(\omega)$ in both 3D and 4D glasses is different from that in 2D glasses. In contrary to 2D glasses, there are less excess modes in larger systems in both 3D and 4D glasses, as conveyed in Figs. 1(b) and 1(c) where $I(\omega)$ decreases as N increases. This numerical observation in 3D and 4D glasses seems to be at odds with the theoretical prediction in Refs. [41,53] where it is expected that $I(\omega)$ should never decrease with increasing N. Further work is needed to understand the notable difference in the finite-size effect observed here across various spatial dimensions.

Currently, figuring out the value of the scaling exponent β in $I(\omega) \sim \omega^{\beta}$ at low frequencies below ω_1 in glasses has become a debated topic.[41,46,48,49] Some numerical studies ar-

gued that $\beta \approx 5$ below ω_l in 2D, 3D, and 4D glasses.[40,41,44] However, there are other studies[17,42,48,49] reporting that $\beta \approx 5$ works conditionally in both 2D and 3D glasses. Specifically, thanks to much lower frequencies being probed in Refs. [17,48,49], it was reported that there is a low-frequency region where $\beta \approx 4.5$ works well in both 2D and 3D glasses, which is independent of the system size and interaction potential model. In addition, the ω^5 scaling could work in some glasses in an intermediate-frequency regime near ω_l but above which the $\omega^{4.5}$ scaling is observed. We indicate two power-law lines of $I(\omega) \sim \omega^{4.5}$ in Fig. 1(a) for 2D glasses and Fig. 1(b) for 3D glasses; however, here we refer the readers to Refs. [17,48,49] where detailed presentations and discussions of the density of excess modes in 2D[17,49] and 3D[48] glasses have been made.

As for in 4D glasses, $I(\omega) \sim \omega^5$ is what the low-frequency excess modes are suggested to follow according to Refs. [41,45]; however, excess modes in the extremely low-frequency regime where the scaling may change if based on studies in 2D and 3D glasses, have not yet been probed in 4D glasses. Therefore, it is necessary to check whether the ω^5 scaling could persist down to much lower frequencies in 4D glasses; if not, whether the power-law scaling of $I(\omega) \sim \omega^{4.5}$ applying to both 2D and 3D glasses could also be a good description to the low-frequency $I(\omega)$ data in 4D glasses.

We show in Fig. 2(a) the ω dependence of the cumulative density of excess modes $I(\omega)$ for systems with sizes $N = 5000$, $N = 20000$, and 100000. We also draw three different types of lines indicating $I(\omega) \sim \omega^4$, $I(\omega) \sim \omega^{4.5}$ and $I(\omega) \sim \omega^5$, respectively, which could provide a preliminary estimate of the applicability of different scaling laws. Though it seems that that every scaling law has its applicability in some frequency range for each N, it is obvious that $I(\omega) \sim \omega^4$ could only work at the lowest frequencies where these data points still seem to depend on the ensemble size. Note that the ensemble size dependence of the several lowest-frequency data points is amplified in reduced plots of $I(\omega)/\omega^\beta$, as shown in Figs. 2(b) and 2(c). Therefore, it requires more data to check whether the $I(\omega) \sim \omega^4$ is possible at very low frequencies, which is now impossible due to the computational capacity. To have a stringent check of the other two scalings, we show reduced plots of $I(\omega)/\omega^\beta$ in Figs. 2(b) and 2(c) since a plateau in the plot of $I(\omega)/\omega^\beta$ will indicate more convincingly $I(\omega) \sim \omega^\beta$.

We first check how the scaling of $I(\omega) \sim \omega^5$ performs at low frequencies by plotting $I(\omega)/\omega^5$ vs. ω in Fig. 2(b). One could observe that there is not any frequency regime where $I(\omega) \sim \omega^5$ could work when N is small, e.g., when $N = 5000$. This could be expected if one assumes that the claim[42] of $I(\omega) \sim \omega^5$ will be observed only when N is large enough in 3D glasses, applies as well to 4D glasses. With N increasing, there is a trend of curve up with increasing ω in the intermediate-frequency regime around $\omega = 0.4$, see, e.g., the plot for $N = 20000$; finally, we could see an apparent intermediate-frequency plateau in our largest system ($N = 100000$) examined, hence suggesting that $I(\omega) \sim \omega^5$ at these frequencies. To our knowledge, the scaling of $I(\omega) \sim \omega^5$ was assumed implicitly to work down to zero frequency in 4D glasses. However, the $I(\omega) \sim \omega^5$ scaling observed in $N = 100000$ could not persist when going down to the lowest-frequency regime we could access, because there is a visible upturn with decreasing ω below the plateau. The scenario observed here in 4D glasses that $I(\omega) \sim \omega^5$ works in some glasses at intermediate frequencies but fails at low frequencies resembles very much that observed in 2D and 3D glasses, which motivates us next to revisit the scaling of $I(\omega)$ in the low-frequency regime where $I(\omega) \sim \omega^5$ is observed to break down.

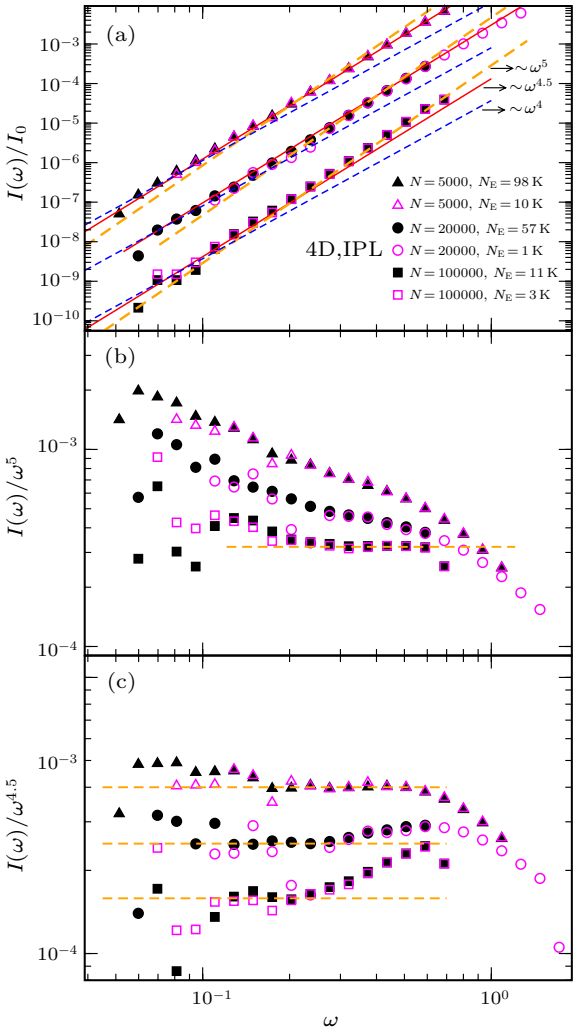


Fig. 2. The cumulative density of states $I(\omega)$ in (a) and corresponding $I(\omega)/\omega^5$ in (b) and $I(\omega)/\omega^{4.5}$ in (c) for 4D IPL model glasses with system sizes $N = 5000$, $N = 20000$, and $N = 100000$. The $I(\omega) \sim \omega^{4.5}$ scaling seems to be a good description to the low-frequency spectrum of excess modes in these system sizes under study. We indicate in (a) the ω^4, $\omega^{4.5}$ and ω^5 power-law lines. The horizontal dashed lines in (b) and (c) serve as a guide to eyes. For each N, data from two different ensemble sizes N_E are shown. Note that $I(\omega)$ in (a) has been scaled by a factor I_0 for visualization purpose: ($I_0 = 0.01$, $N = 5000$), ($I_0 = 0.1$, $N = 20000$) and ($I_0 = 1$, $N = 100000$).

One natural candidate of the scaling at the lowest frequencies in 4D glasses is $I(\omega) \sim \omega^{4.5}$ since this scaling is followed by excess modes in both 2D and 3D glasses,[17,48,49] which is also the reason why we show lines indicating $I(\omega) \sim \omega^{4.5}$ in Fig. 2(a). We thus plot $I(\omega)/\omega^{4.5}$ vs. ω in Fig. 2(c), and a low-frequency plateau in each plot for N could be observed. This suggests that the $I(\omega) \sim \omega^{4.5}$ scaling is followed by low-frequency excess modes in 4D glasses, independent of system sizes.

Taken together with the results in 2D and 3D glasses,[17,48,49] it seems that scenarios regarding the scaling of the density of excess modes at low frequencies below the first phonon-like mode in 2D, 3D, and 4D glasses are the same. We note that much more configurations are needed to smooth the lowest-frequency $I(\omega)$ data in 4D glasses. Additionally, we could not exclude the possibility that there may be a scaling of, e.g., $I(\omega) \sim \omega^4$ as shown in Fig. 2(a), different from the scaling of $I(\omega) \sim \omega^{4.5}$ at much lower frequencies than we could probe, which, on the other hand, presents the difficulty in the numerical determination of the scaling of $I(\omega)$ at low frequencies.

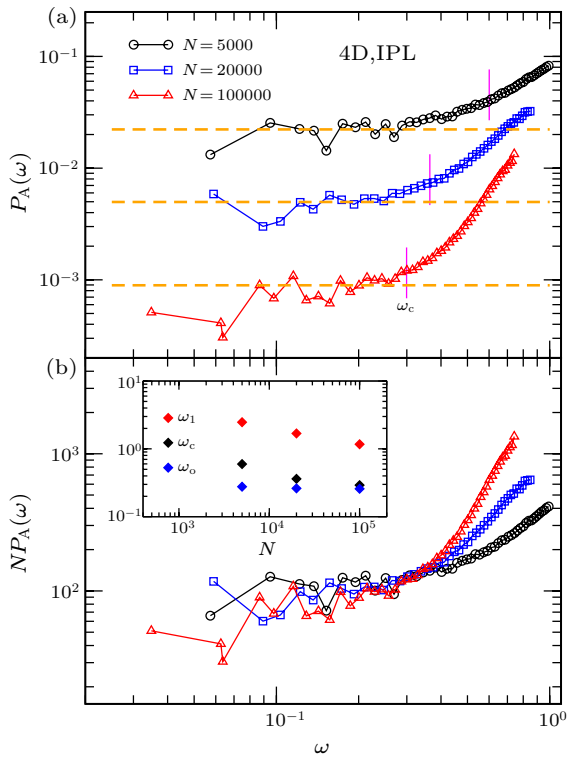


Fig. 3. (a) Frequency ω dependence of the average participation ratio $P_A(\omega)$ for the 4D IPL model glasses with different system sizes N. At low frequencies examined, $P_A(\omega)$ tends to approach a plateau whose value depends on N. (b) $NP_A(\omega)$ vs. ω for the same data in (a). $P_A(\omega)$ scales approximately with N^{-1} at low frequencies. The inset of (b) shows the N dependence of ω_1, ω_c and ω_o. Here, ω_1 is the frequency of the first phonon-like mode, ω_c is the upper frequency cutoff of the low-frequency $\omega^{4.5}$ scaling presented in Fig. 2, and ω_o is the upper frequency cutoff of the low-frequency plateau of $P_A(\omega)$. Ensemble sizes N_E used to obtain $P_A(\omega)$ are $N_E = 10$ K for $N = 5000$, $N_E = 10$ K for $N = 20000$, and $N_E = 6.4$ K for $N = 100000$.

Moreover, we proceed to characterize the spatial localization of excess modes in 4D glasses at very low frequencies, particularly where $I(\omega) \sim \omega^{4.5}$. The mode localization could usually be quantified by the participation ratio $P(\omega_l) = \frac{(\sum_{i=1}^{N} |e_{l,i}|^2)^2}{N \sum_{i=1}^{N} |e_{l,i}|^4}$, where $e_{l,i}$ is the polarization vector pertaining to particle i in the mode l. A localized mode has a small value of participation ratio, whereas a large value of participation ratio is indicative of an extended mode. Like in 3D glasses,[48] we find that the participation ratio of different modes exhibits significant fluctuations as well in 4D glasses; therefore, as suggested in Refs. [41,48], we check the frequency dependence of the average participation ratio $P_A(\omega)$ in Fig. 3(a). $P_A(\omega)$ decreases with decreasing ω at intermediate ω, and converges approximately to a low-frequency plateau when ω decreases below around the frequency $\omega_o \approx 0.27$ in all the three systems studied. However, the height of the low-frequency plateau depends on N.

We then compare in the inset of Fig. 3(b), ω_o, ω_1 (the frequency of the first phonon-like mode), and ω_c (the upper frequency cutoff of the low-frequency $\omega^{4.5}$ scaling presented in Fig. 2). Here $\omega_c > \omega_o$ in all the three system sizes, but ω_c decreases and approaches ω_o when N increases. Additionally, both ω_c and ω_o lie significantly below ω_1. Future work will check whether $\omega_o > \omega_c$ could be observed in larger systems. In addition, we show in Fig. 3(b) the plot of $NP_A(\omega)$ vs. ω to check whether the reported relation[41] of $P_A(\omega) \sim N^{-1}$ could persist at much lower frequencies where $I(\omega) \sim \omega^{4.5}$. This relation seems to work, though there are large fluctuations (possibly due to statistics) in the low-frequency data collapse.

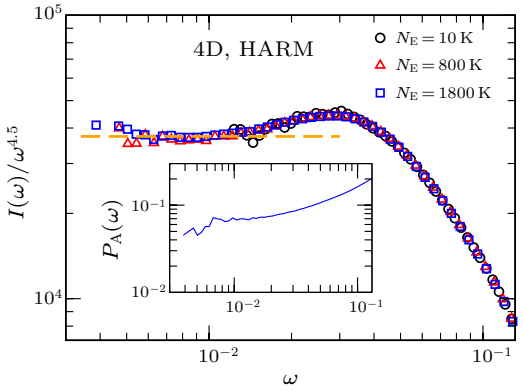


Fig. 4. (a) The reduced cumulative density of states $I(\omega)/\omega^{4.5}$ for 4D HARM model glasses with $N = 1024$. The inset shows the average participation ratio $P_A(\omega)$ vs. ω.

Finally, to check the interaction potential model dependence of the low-frequency scaling of $I(\omega) \sim \omega^{4.5}$ in 4D model glasses, we calculated $I(\omega)$ in the 4D HARM model glasses with ensemble sizes up to about two million. As demonstrated in Fig. 4, the plot of $I(\omega)/\omega^{4.5}$ vs. ω is a plateau at the lowest frequencies, thus supporting the robustness of the scaling of $I(\omega) \sim \omega^{4.5}$ across different interaction potential models. Moreover, the upper frequency cutoff ω_c of this scaling seems to be around the onset frequency ω_o, below which

the average participation ratio $P_A(\omega)$ is approximately constant, see the inset in Fig. 4. However, we note that ω_o does not need to coincide with ω_c if taking into account results from 4D IPL model glasses in the inset to Fig. 3(b), where ω_c could be visibly different from ω_0. Note that the absolute value of the characteristic frequencies, e.g., ω_c and ω_0, depends largely on potential models and densities (or pressures).

4. Summary and outlook

In conclusion, we have conducted computer simulation studies of the low-frequency excess modes significantly below the first phonon-like mode. We observe an increase in the density of excess modes at frequencies below the first phonon-like mode in 2D glasses but a decrease in both 3D and 4D glasses as the system size increases. This thus suggests that the dependence of the excess mode density on system sizes varies with spatial dimensions, warranting further investigation. Importantly, we find the density of excess modes in the lowest-frequency regime accessed scales with $\omega^{3.5}$ instead of the previously reported ω^4 in 4D glasses;[41] the ω^4 scaling could work but conditionally. Moreover, we demonstrate that the low-frequency $\omega^{3.5}$ scaling is independent of system sizes and interaction potential models examined. Taken together with the observation of the $\omega^{3.5}$ scaling at low frequencies below the first phonon-like mode in both 2D and 3D glasses,[17,48,49] our findings indicate that this low-frequency scaling exhibits robustness across different spatial dimensions.

Our work raises several open questions. First, will the glass stability influence the low-frequency $\omega^{3.5}$ scaling of the spectrum of excess modes in 4D glasses as well as 3D glasses? The $\omega^{3.5}$ scaling was reported to be independent of the glass stability in 2D glasses,[49] and it is then interesting to check whether this could persist in other spatial dimensions. Second, is the low-frequency $\omega^{3.5}$ scaling in 4D glasses (including in 2D and 3D glasses) due to finite-size effects? It is difficult to answer it in simulations, but future theoretical work may shed light on this. Third, will the stress distribution affect the low-frequency scaling of the density of excess modes in 4D glasses as it does in 2D and 3D glasses?[47] Fourth, how about the scaling of the density of excess modes hybridizing with phonon-like modes in 4D glasses? Previous observations[17,48,49] in 2D and 3D glasses tell us that the density of excess modes hybridizing with phonon-like modes differs from that of excess modes not hybridizing with phonon-like modes. Therefore, it is imperative to directly investigate the scaling behavior of hybridized excess modes in 4D glasses, which we find, however, poses significant computational challenges at present if using the method of diagonalizing dynamical matrix. Future work will check whether the method of using the Fourier transformation of the velocity correlation functions[54,55] to get the density of states could help in dealing with this issue. Finally, will the low-frequency $\omega^{3.5}$ scaling of the density of excess modes in 4D glasses as well as in 2D and 3D glasses survive when going to much lower frequencies? This poses another computation challenge. Actually, the inability to determine in simulations the scaling behavior of excess modes at low enough frequencies also constitutes an obstacle to the numerical investigation of properties of excess modes. Future work should also check how the anharmonicty induced by thermal excitations affects the scaling of the density of excess modes, which is more related to realistic experiments. The Fourier transformation of the velocity correlation functions should be a good tool to use when studying this.

Acknowledgments

We thank G. Szamel and E. Flenner for discussions on properties of 4D glasses. We also thank E. Flenner for providing feedback on an early version of our manuscript. We acknowledge the support from the National Natural Science Foundation of China (Grant Nos. 12374202 and 12004001), Anhui Projects (Grant Nos. 2022AH020009, S020218016, and Z010118169), and Hefei City (Grant No. Z020132009). We also acknowledge Hefei Advanced Computing Center, Beijing Super Cloud Computing Center, and the High-Performance Computing Platform of Anhui University for providing computing resources.

References

[1] Kittel C 1996 *Introduction to Solid State Physics* 7th edn. (New York: Wiley)
[2] Zeller R C and Pohl R O 1971 *Phys. Rev. B* **4** 2029
[3] Anderson P W, Halperin B I and Varma C M 1972 *Philos. Mag.* **25** 1
[4] Pohl R O, Liu X and Thompson E 2002 *Rev. Mod. Phys.* **74** 991
[5] Phillips W A 1972 *J. Low Temp. Phys.* **7** 351
[6] Xu N, Vitelli V, Wyart M, Liu A J and Nagel S R 2009 *Phys. Rev. Lett.* **102** 038001
[7] Flenner E, Wang L and Szamel G 2020 *Soft Matter* **16** 775
[8] Chen K, Manning M L, Yunker P J, Ellenbroek W G, Zhang Z, Liu A J and Yodh A G 2011 *Phys. Rev. Lett.* **107** 108301
[9] Xu N, Vitelli V, Liu A J and Nagel S R 2010 *Europhys. Lett.* **90** 56001
[10] Malandro D L and Lacks D J 1999 *J. Chem. Phys.* **110** 4593
[11] Manning M L and Liu A J 2011 *Phys. Rev. Lett.* **107** 108302
[12] Tong H and Xu N 2014 *Phys. Rev. E* **90** 010401
[13] Maloney C E and Lemaitre A 2004 *Phys. Rev. Lett.* **93** 195501
[14] Wang L, Duan Y and Xu N 2012 *Soft Matter* **8** 11831
[15] Widmer-Cooper A, Perry H, Harrowell P and Reichman D R 2008 *Nat. Phys.* **4** 711
[16] Wang L and Xu N 2014 *Phys. Rev. Lett.* **112** 055701
[17] Wang L, Szamel G and Flenner E 2021 *Phys. Rev. Lett.* **127** 248001
[18] Fu L, Zheng Y and Wang L 2024 *Chin. Phys. B* **33** 056401
[19] Wang L, Berthier L, Flenner E, Guan P and Szamel G 2019 *Soft Matter* **15** 7018
[20] Bouchbinder E, Lerner E, Rainone C, Urbani P and Zamponi F 2021 *Phys. Rev. B* **103** 174202
[21] Folena G and Urbani P 2022 *J. Stat. Mech.* **2022** 053301
[22] Shimada M and De Giuli E 2022 *SciPost Phys.* **12** 090
[23] Stanifer E, Morse P K, Middleton A A and Manning M L 2018 *Phys. Rev. E* **98** 042908
[24] Shimada M, Mizuno H and Ikeda A 2020 *Soft Matter* **16** 7279
[25] Gurevich V L, Parshin D A and Schober H R 2003 *Phys. Rev. B* **67** 094203

[26] Schirmacher W, Ruocco G and Scopigno T 2007 *Phys. Rev. Lett.* **98** 025501
[27] Xu N, Liu A J and Nagel S R 2017 *Phys. Rev. Lett.* **119** 215502
[28] Buchenau U, Galperin Yu M, Gurevich V L, Parshin D A, Ramos M A and Schober H R 1992 *Phys. Rev. B* **46** 2798
[29] Gurarie V and Chalker J T 2003 *Phys. Rev. B* **68** 134207
[30] Tanguy A, Wittmer J P, Leonforte F and Barrat J L 2002 *Phys. Rev. B* **66** 174205
[31] Leonforte F, Boissière R, Tanguy A, Wittmer J P and Barrat J L 2005 *Phys. Rev. B* **72** 224206
[32] Lerner E, DeGiuli E, Düring G and Wyart M 2014 *Soft Matter* **10** 5085
[33] Mizuno H, Shiba H and Ikeda A 2017 *Proc. Natl. Acad. Sci. USA* **114** E9767
[34] Wang L, Ninarello A, Guan P, Berthier L, Szamel G and Flenner E 2019 *Nat. Commun.* **10** 26
[35] Gartner L and Lerner E 2016 *Sci. Post Phys.* **1** 016
[36] Wijtmans S and Manning M L 2017 *Soft Matter* **13** 5649
[37] Angelani L, Paoluzzi M, Parisi G and Ruocco G 2018 *Proc. Natl. Acad. Sci. USA* **115** 8700
[38] Shiraishi K, Hara Y and Mizuno H 2022 *Phys. Rev. E* **106** 054611
[39] Shiraishi K, Mizuno H and Ikeda A 2023 *J. Chem. Phys.* **158** 174502
[40] Lerner E, Düring G and Bouchbinder E 2016 *Phys. Rev. Lett.* **117** 035501
[41] Kapteijns G, Bouchbinder E and Lerner E 2018 *Phys. Rev. Lett.* **121** 055501
[42] Lerner E 2020 *Phys. Rev. E* **101** 032120
[43] Das P, Hentschel H G E, Lerner E and Procaccia I 2020 *Phys. Rev. B* **102** 014202
[44] Richard D, González-López K, Kapteijns G, Pater R, Vaknin T, Bouchbinder E and Lerner E 2020 *Phys. Rev. Lett.* **125** 085502
[45] Shimada M, Mizuno H, Berthier L and Ikeda A 2020 *Phys. Rev. E* **101** 052906
[46] Lerner E and Bouchbinder E 2022 *J. Chem. Phys.* **157** 166101
[47] Krishnan V V, Ramola K and Karmakar S 2022 *Soft Matter* **18** 3395
[48] Wang L, Fu L and Nie Y 2022 *J. Chem. Phys.* **157** 074502
[49] Wang L, Szamel G and Flenner E 2023 *J. Chem. Phys.* **158** 126101
[50] Mocanu F C, Berthier L, Ciarella S, Khomenko D, Reichman D R, Scalliet C and Zamponi F 2023 *J. Chem. Phys.* **158** 014501
[51] Paoluzzi M, Angelani L, Parisi G and Ruocco G 2019 *Phys. Rev. Lett.* **123** 155502
[52] Bitzek E, Koskinen P, Gähler F, Moseler M and Gumbsch P 2006 *Phys. Rev. Lett.* **97** 170201
[53] Lerner E and Bouchbinder E 2018 *J. Chem. Phys.* **148** 214502
[54] Wang L and Xu N 2013 *Soft Matter* **9** 2475
[55] Keyes T 1997 *J. Phys. Chem. A* **101** 2921